PROCEEDINGS OF SCIENCE

Measurement of the inclusive photon and photon+jet production cross-sections at $\sqrt{s}$ = 7 TeV with the ATLAS detector and constraints to PDFs

Matthias Saimpert on behalf of the ATLAS Collaboration*
CEA Saclay - Irfu/SPP
E-mail: matthias.saimpert@cern.ch

Measurements of inclusive photon production performed by the ATLAS collaboration using an integrated luminosity of 4.6 fb^{-1} are reported as a function of the photon transverse energy in different fiducial regions covering a wide acceptance. A comparison to the data of the next-to-leading order QCD calculation using JETPHOX program with different PDFs is presented. The impact of the measurements to constrain the gluon PDF is also evaluated. The cross sections for photons produced in association with a jet are also measured using an integrated luminosity of 37 pb^{-1} as functions of photon and jet kinematics and are compared to the JETPHOX calculation. The theoretical uncertainties, including scale, strong coupling, and PDF uncertainties are evaluated for all predictions. Data and theory typically show a good agreement within uncertainties, except for the azimuthal angle in the photon + jet case.

The XXIII International Workshop on Deep Inelastic Scattering and Related Subjects
April 27 - May 1, 2015
Southern Methodist University
Dallas, Texas 75275

*Speaker.

PoS(DIS2015)155

ATL-PHYS-PROC-2015-046
10 July 2015

1. Introduction

In proton-proton (pp) collisions at the LHC [1], photons are produced mainly by three different mechanisms. The first category of interest are photons coming directly from the hard parton scattering, called direct photons, which are direct probes of perturbative QCD (pQCD) as shown in Figure 1 (left, middle). However, photons can also originate from parton fragmentation (Figure 1, right) or from hadron or tau lepton decays. In the following, direct and fragmentation photons are designated as prompt photons whereas the other ones are excluded from both measurements and theoretical predictions.

The measurement of inclusive prompt photon ($pp \to \gamma + X$) and photon + jet ($pp \to \gamma + jet + X$) production provides a valuable tool to test pQCD. Indeed, higher order effects are expected to play an important role and the full Next-To-Leading Order (NLO) calculation JETPHOX is available to test the predictions at NLO [2, 3]. Furthermore, many Higgs boson studies and Beyond Standard Model (BSM) searches at the LHC look at photon final states, which then need to be well understood in the context of the Standard Model. As an example, the photon + jet process is the main reducible background to $H \to \gamma\gamma$ studies [4]. In addition, those measurements can be used to study parton fragmentation for instance by investigating the dynamics of the underlying process in photon + jet events, and to constrain the gluon density function in the proton since the main production mechanism of $\gamma + X$ at the LHC is via $qg \to q\gamma$ (see Figure 1, left).

This document starts by presenting in Section 2 the measurement of the inclusive isolated prompt photon production at $\sqrt{s}$ = 7 TeV done by the ATLAS collaboration [5] with an integrated luminosity of 4.6 fb^{-1} [6]. Event selection, Monte Carlo (MC) simulation samples, residual background estimation, unfolding and uncertainties are described and final results with comparisons to NLO theoretical predictions are shown. The sensitivity of this measurement to the proton parton distributions is also reported [7]. Then, the photon + jet measurement performed with the ATLAS detector at the center-of-mass energy $\sqrt{s}$ = 7 TeV but with an integrated luminosity of 37 pb^{-1} [8] is presented in Section 3 following the same procedure. Finally, conclusions and prospects for those two measurements are given in Section 4.

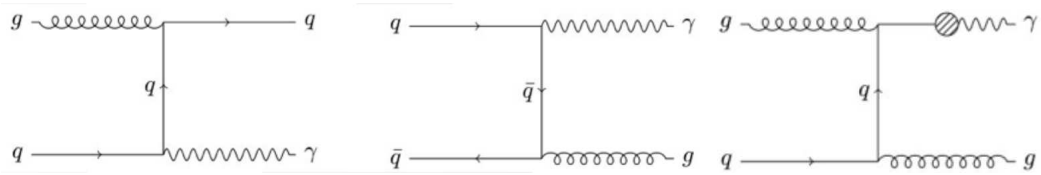

Figure 1: Main inclusive prompt photon production mechanisms in pp collisions at the LHC: direct (left, middle) and fragmentation (right).

2. Measurement of inclusive isolated prompt photon production

2.1 Event selection and Monte Carlo simulations

The measurement presented in this section is based on 4.6 fb^{-1} of pp collision data collected in 2011 at a center-of-mass of $\sqrt{s}$ = 7 TeV by the ATLAS detector at the LHC and reported in [6]. $pp \to \gamma + X$ final states are triggered using an unprescaled photon trigger with a nominal photon

transverse momentum (E_T^γ) threshold of 80 GeV. Quality cuts are applied in order to select good collision data and events containing at least one reconstructed photon candidate with $E_T^\gamma > 100$ GeV and pseudorapidity (η^γ) satisfying $|\eta^\gamma| < 1.37$ or $1.52 < |\eta^\gamma| < 2.37$.

After this first selection, a very important hadronic background coming from boosted meson decays such as $\pi^0 \to \gamma\gamma$ is still present in the sample. In order to further reject those events, additional cuts on the photon shower shape profiles, called photon tight identification requirements, and on the photon transverse isolation energy ($E_T^{iso} < 7$ GeV) are implemented. The photon transverse isolation energy is computed as the scalar sum of the electromagnetic calorimeter cell transverse energies within a cone of radius $\Delta R = 0.4$ around the photon candidate, corrected for the photon contribution and pile up/underlying event effects. After the full selection, the data sample contains about 1 million central events ($|\eta^\gamma| < 1.37$) and half a million forward events ($1.52 < |\eta^\gamma| < 2.37$).

The MC programs PYTHIA 6.4 [9] and HERWIG 6.5 [10] are used to generate signal events. The event-generator parameters, including those of the underlying-event modelling, were set according to the AMBT2 [12] and AUET2 [13] tunes for PYTHIA and HERWIG, respectively. Both generators make use of the modified leading order MRST2007 [11] Parton Density Function (PDF) set.

2.2 Residual background estimation, unfolding and main measurement uncertainties

After the full event selection, the residual background from boosted $\pi^0 \to \gamma\gamma$ is still large, contaminating up to 6% of the events at low E_T^γ. In order to estimate it, the so-called two-dimensional sideband method is used as in the previous analysis [14]. Several cuts on the photon shower shape profiles are reversed in order to define a background control region, and photon identification and isolation energy are assumed to be uncorrelated. The hadronic event component is then estimated and subtracted in each E_T^γ bin, separately for the central and forward regions. The proportion of signal events in E_T^γ bins is shown in Figure 2 (left) with statistical uncertainties. Alternative background subtraction methods lead to differences of 2 to 3% on the cross-sections, which is taken as a systematic uncertainty. A small background coming from electrons misreconstructed as photons is also present (0.5% for $E_T^\gamma < 400$ GeV) and subtracted using a data-driven technique based on a Z mass peak study.

The measured cross section is then unfolded from detector effects using bin by bin correction factors following Equation 2.1:

$$(\frac{d\sigma}{d\mathscr{O}})_i = \frac{N_i^{obs.} - N_i^{bkg.}}{C_i^{MC} \Delta\mathscr{O} \mathscr{L}} \quad ; \quad C_i^{MC} = \frac{N_{i,reconstructed}^{MC}}{N_{i,generated}^{MC}} \tag{2.1}$$

$(\frac{d\sigma}{d\mathscr{O}})_i$ is the differential cross section for the observable $\mathscr{O}$ in the i^{th} bin, $N_i^{obs.}$ and $N_i^{bkg.}$ are the number of observed and estimated background events in the i^{th} bin, C_i^{MC} is the correction factor, $\Delta\mathscr{O}$ the bin width and $\mathscr{L}$ the integrated luminosity. The correction factors are computed from the MC signal samples as the ratio of signal events passing the selection at reconstructed level to all generated signal events. They take into account acceptance and smearing effects, identification, isolation and trigger efficiencies. MC samples are corrected in a previous step to match data efficiencies [15]. The dominant systematic uncertainties on the correction factors come from the photon energy scale (2 to 6% from low to high E_T^γ) and the choice of the MC generator (PYTHIA

or HERWIG, 2 to 4% from low to high E_T^γ). The ATLAS data luminosity uncertainty of the considered dataset is 1.8% [16]. The correction factors and their total uncertainties are shown in the different E_T^γ bins for the central and forward regions in Figure 2 (right). As one can see, their values go from 0.8 to 1 so that the size of the corrections is in general pretty small. Uncertainties on the correction factors are added in quadrature and all uncertainties (background subtraction, correction factors, luminosity) are propagated to the final results using Equation 2.1.

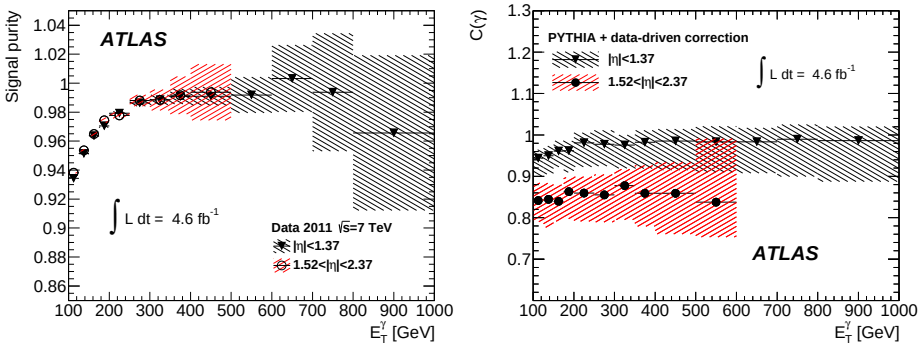

Figure 2: Signal purity (left) and bin by bin correction factors (right) in E_T^γ bins for the central and forward regions. Uncertainties are statistical only for the left plot whereas total uncertainties are shown on the right plot [6].

2.3 Theoretical predictions and final results

Theoretical predictions are computed using the JETPHOX MC program [2, 3], which implements a full NLO calculation at $O(\alpha\alpha_s^2)$ for both direct and fragmentation photon components. The fiducial selection is the same than the one in data, so only events with at least a photon with $E_T^\gamma > 100$ GeV and $|\eta^\gamma| < 1.37$ or $1.52 < |\eta^\gamma| < 2.37$ are kept. A parton level isolation cut is also implemented in a cone $\Delta R = 0.4$, $E_T^{parton\ iso} < 7$ GeV. The transverse isolation energy computed at parton level is corrected for pile up and underlying event residual effects to match better the cut applied at reconstructed level by using PYTHIA and HERWIG parton showers. JETPHOX uses the fragmentation function BFG set II [17] in its calculation and the renormalization, factorization and fragmentation scales are all set to E_T^γ. The Parton Density Function (PDF) sets used to compute the predictions are CT10 [18] and MSTW2008nlo [19]. The theoretical uncertainties are estimated by varying the three scales together to $E_T^\gamma/2$ and $2 \times E_T^\gamma$ (from 12 to 20% effect, leading uncertainty), the eigenvectors of CT10 PDFs within their uncertainties (5 to 15% from low to high E_T^γ), and the strong coupling constant α_s in the range of 0.118 ± 0.002 (4.5% effect with a small E_T^γ dependence). All uncertainties are added in quadrature and quoted as the theoretical uncertainty.

The total fiducial cross section measurement is:

$$\sigma_{exp.}(\gamma+X) = 236 \pm 2(stat.) \pm^{+13}_{-9} (syst.) \pm 4(lumi.)\ \text{pb} \tag{2.2}$$

The JETPHOX prediction for the same fiducial volume when using CT10 (MSTW2008nlo) PDF sets is:

$$\sigma_{th.}(\gamma+X) = 203(212) \pm 25(24)\ \text{pb} \tag{2.3}$$

Both predictions are compatible with the measurement within uncertainties. The measured differential cross section in E_T^γ bins for the central and forward regions are presented together with comparisons to the JETPHOX prediction in Figure 3. JETPHOX is always in agreement with data within uncertainties, even if the predictions show a tendency to be lower than data at low E_T^γ. One can notice that the use of MSTW2008nlo PDF sets leads to a rise of the predictions by about 5% compared to CT10. The total experimental uncertainties are below 6% (7%) in the central (forward) region whereas the theoretical uncertainties, largely dominated by the scale uncertainty, are always above 10%. PYTHIA gives a fair description of data while HERWIG underestimates data by 10-20%.

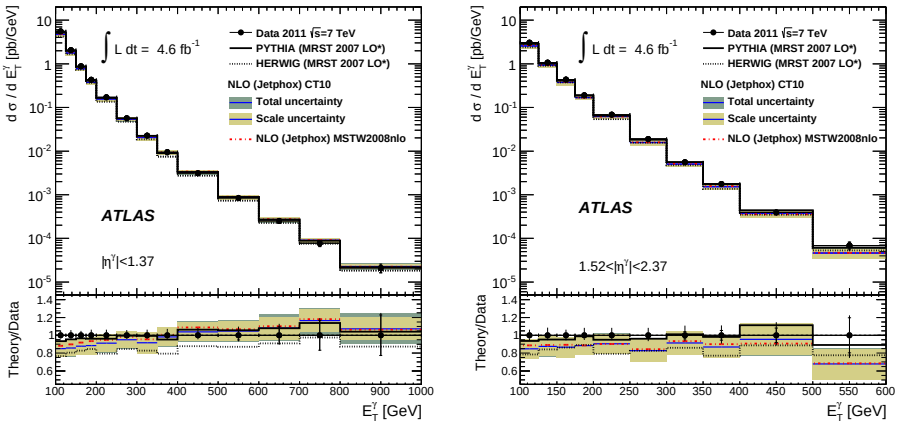

Figure 3: Measured differential inclusive photon cross section in E_T^γ bins in the central (left) and forward (right) region. Points represent the measurement and lines the different theoretical predictions. Error bars are the total experimental uncertainties and error bands represent the theoretical uncertainties for JETPHOX calculation [6].

2.4 Sensitivity to parton density distributions

Inclusive photon production is dominated by the $qg \to q\gamma$ sub-process at the LHC (see Figure 1, left), so shows sensitivity to the gluon PDF. It has been demonstrated to have the potential to constrain the gluon PDF when the proton momentum carried by the gluon is high, the so-called high x region [20]. The ATLAS collaboration studied this sensitivy in [7] and some results are shown in Figure 4. The sensitivity of the measurement to the gluon PDF at high x is observed, nevertheless the scale uncertainty from theory limits the final sensitivity and no PDF sets are clearly favoured by data. A Next-to-Next-Leading Order (NNLO) prediction for this cross section would probably be very helpful in order to take full benefit of the measurement.

3. Dynamics of isolated-photon + jet production

3.1 Event selection, photon + jet observables and Monte Carlo simulations

The measurement presented in this section is based on 37 pb^{-1} of pp collision data collected in 2010 at a center-of-mass of $\sqrt{s}$ = 7 TeV by the ATLAS detector at the LHC and reported in [8]. Additional motivations compared to the measurement presented in Section 2 include a check of the

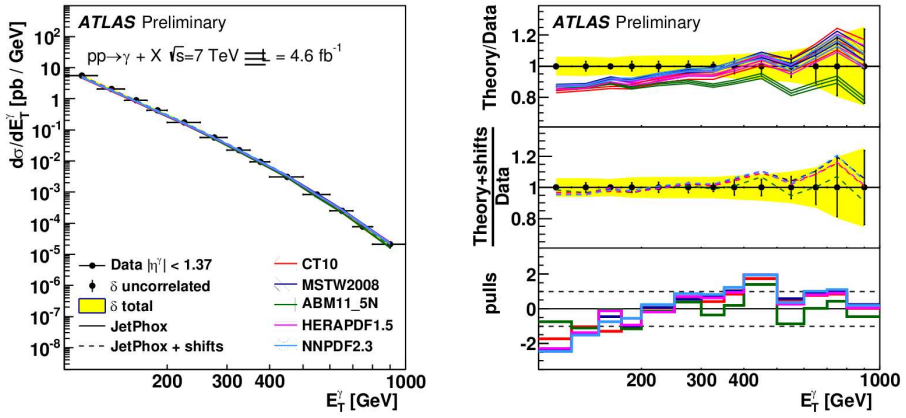

Figure 4: (left) Measurement of the inclusive photon cross section (dots) [6] and JETPHOX predictions (lines) computed with different PDF sets and associated uncertainties. (right) Ratio of theory to data for the different PDF cases and associated pull distributions [7].

main reducible background to $H \rightarrow \gamma\gamma$ and a study of the angular correlations between photons and jets, for MC tuning. $pp \rightarrow \gamma + jet + X$ final states are triggered using an unprescaled photon trigger with a nominal E_T^γ threshold of 40 GeV in order to keep a phase space close enough to the one associated to the Higgs boson decaying to photon pairs. The photon candidate selection is similar to the one used for the inclusive photon measurement with the exception of the E_T^γ cut, which is lowered to 45 GeV. The isolation requirement is also optimized for this analysis and $E_T^{iso.} < 3$ GeV in a cone of $\Delta R = 0.4$ is required. At least one jet reconstructed with the anti-k_t algorithm [21] with a distance parameter R = 0.6, transverse momentum $p_T^{jet} > 40$ GeV and rapidity $|y^{jet}| < 2.37$ is required. Events where the jet is too close to the photon ($\Delta R^{\gamma\ jet} < 1$) are excluded. After the full selection, the sample contains about 124,000 events.

The studied variables include E_T^γ, p_T^{jet} and $|y^{jet}|$ for pQCD checks and the azimuthal angle between the photon and the jet $\Delta\phi^{\gamma jet}$, the photon-jet invariant mass $m^{\gamma\ jet}$ and $|\cos\theta^{\gamma jet}|$, where $\theta^{\gamma jet}$ corresponds to the scattering angle in the parton center-of-mass frame, for correlation measurements. $|\cos\theta^{\gamma jet}| = |\tanh(\Delta y/2)|$ is of special interest because its shape is directly related to the spin of the exchanged particle in case of t channel processes. It is especially useful for disentangling direct and fragmentation components at Leading Order (LO) since fragmentation is the only component which can be produced by gluon exchanged at LO.

3.2 Residual background estimation, unfolding and main measurement uncertainties

The residual background estimation and unfolding technique are similar to the ones reported in Section 2.2. The background can be up to 10% of the events at low E_T^γ and the uncertainty on the signal yield is 2%. Bin by bin correction factors are used for unfolding. In the case of $|\cos\theta^{\gamma jet}|$, the main uncertainties arise from the jet energy scale (5%) and the detector material uncertainties (5%). The ATLAS data luminosity uncertainty of the considered dataset is 3.4%.

3.3 Theoretical predictions and final results

Similarly to Section 2.3, the JETPHOX MC program is used to compute theoretical predic-

tions. In the case of $|\cos\theta^{\gamma jet}|$, the scale uncertainty is 14%, PDF uncertainties 3.5% and α_s uncertainty 2.5%.

A selection of the cross section measurements reported in [8] are shown in Figure 5. Some extra kinematical selection is applied in the case of $|\cos\theta^{\gamma jet}|$ in order not to bias the phase space. A good agreement is observed between NLO theory and data, except for the azimuthal angle between the photon and the jet. This can be explained by the fact that partonic level NLO generators like JETPHOX produce only two and three body final states, so if one selects the photon and the leading jet one cannot find an azimuthal angle between them below $\frac{\pi}{2}$. On the other hand, PYTHIA and SHERPA MC, which are LO generators with parton shower do a fairly good job at describing data. HERWIG underestimates the data by up to 50%.

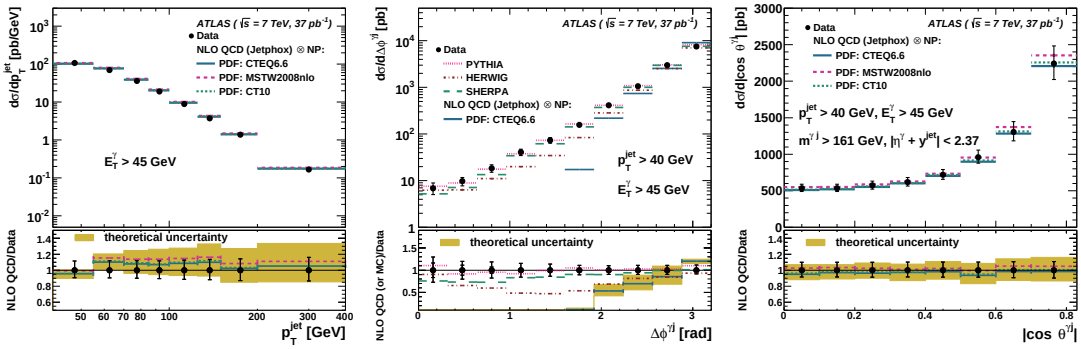

Figure 5: Measured differential inclusive photon + jet cross section with respect to the jet transverse momentum (left), the azimuthal angle between photon and jet (middle) and $|\cos\theta^{\gamma jet}|$ (right). Points represent the measurement and lines the different theoretical predictions. Error bars are the total experimental uncertainties and error bands represent the theoretical uncertainties for JETPHOX calculation [8].

4. Conclusion

The measurement of the inclusive photon and photon + jet cross section in pp collisions at $\sqrt{s}$ = 7 TeV with the ATLAS detector have been reported. In general, NLO predictions are in agreement with the measurements within uncertainties. However, the theoretical scale uncertainty is often dominant which decreases the impact of those measurements. Indeed the inclusive photon measurement has been demonstrated to have a good potential to constraint the gluon PDFs at high x and would highly benefit from updated predictions with reduced uncertainties. Studying the dynamics of photon + jet events allow for checks of the main reducible background to $H \rightarrow \gamma\gamma$ studies and the validity of the parton shower models used in the LO MC generators. While the azimuthal angle between the photon and the leading jet requires at least a partonic NNLO calculation or parton shower modelling to be described accurately, due to the opening of phase space, all the other variables which were studied are well described by the NLO pQCD JETPHOX calculation.

References

[1] L. Evans and P. Bryant, JINST **3**, S08001 (2008).

[2] S. Catani, M. Fontannaz, J. P. Guillet and E. Pilon, JHEP **0205**, 028 (2002).

[3] P. Aurenche, M. Fontannaz, J. P. Guillet, E. Pilon and M. Werlen, Phys. Rev. D **73**, 094007 (2006).

[4] ATLAS and CMS Collaborations, Phys. Rev. Lett. **114**, 191803 (2015).

[5] ATLAS Collaboration, JINST **3**, S08003 (2008).

[6] ATLAS Collaboration, Phys. Rev. D **89**, no. 5, 052004 (2014).

[7] ATLAS Collaboration, ATL-PHYS-PUB-2013-018, http://cds.cern.ch/record/1636863.

[8] ATLAS Collaboration, Nucl. Phys. B **875**, 483 (2013).

[9] T. Sjostrand, S. Mrenna and P. Z. Skands, JHEP **0605**, 026 (2006).

[10] G. Corcella *et al.*, JHEP **0101**, 010 (2001).

[11] A. D. Martin, R. G. Roberts, W. J. Stirling and R. S. Thorne, Eur. Phys. J. C **4**, 463 (1998).

[12] ATLAS Collaboration, ATL-PHYS-PUB-2011-009, http://cds.cern.ch/record/1363300.

[13] ATLAS Collaboration, ATL-PHYS-PUB-2011-008, http://cds.cern.ch/record/1345343.

[14] ATLAS Collaboration, Phys. Lett. B **706**, 150 (2011).

[15] ATLAS Collaboration, ATLAS-CONF-2012-123, http://cds.cern.ch/record/1473426.

[16] ATLAS Collaboration, Eur. Phys. J. C **73**, no. 8, 2518 (2013).

[17] L. Bourhis, M. Fontannaz and J. P. Guillet, Eur. Phys. J. C **2**, 529 (1998).

[18] H. L. Lai *et al.*, Phys. Rev. D **82**, 074024 (2010).

[19] A. D. Martin, W. J. Stirling, R. S. Thorne and G. Watt, Eur. Phys. J. C **63**, 189 (2009).

[20] D. d'Enterria and J. Rojo, Nucl. Phys. B **860**, 311 (2012).

[21] M. Cacciari, G. P. Salam and G. Soyez, JHEP **0804**, 063 (2008).

PoS(DIS2015)155